

the number of the water molecules in attractive interactions is lower by 3 than those for tGg'. Thus it is concluded for the conformers studied here that the number of the waters hydrogen bonding to the solute is a more important parameter in defining the sign of  $\Delta E_{SX}$  and of  $\Delta G$  than the number of the water molecules in attractive interactions. For the tGt conformer the two effects act in the same direction, resulting in considerable stabilization by 8.4 kcal/mol for  $\Delta E_{SX}$  and by 3.4 kcal/mol for  $\Delta G$ .

While trends in  $\Delta E_{SX}$  and  $\Delta G$  are in line with the solution structure parameters, no correlation to these parameters was found considering the  $\Delta H$ ,  $T\Delta S$ , and  $\Delta E_{SS}$  (solvent reorganization) terms in Table VI. The values obtained by direct comparison of the  $H$  values for solutions after considering 4500K configurations show large relative errors for the  $\Delta H$ ,  $T\Delta S = \Delta H - \Delta G$ , and  $\Delta E_{SS} = \Delta H - \Delta E_{SX}$  terms. These errors make uncertain even the sign of the above terms for the tGg and tGt conformers. Results obtained in the perturbation calculations showed poorly converged values after considering 3000K configurations in the subsequent steps. Despite the uncertainty in the  $T\Delta S$  values for tGt and gGg, more positive entropy, thus a less ordered solution structure, is expected when the solute is in the tGt rather than in the gGg conformation. On the contrary, the radial distribution functions are similar around the first peaks for these conformers (Figures 2-4 and 9). The number of hydrogen bonds to the solute and the number of the water molecules in the first hydration shell, where the water molecules are expected to be strongly bound to the solute, are larger for tGt than gGg (Table V). This suggests a more ordered structure for tGt, contrary to the above interpretation of the entropy values. So we consider the calculated entropy difference as characterizing the differences in the bulk solution

structure and not directly correlating with the first hydration shell structure parameters. The effect that dominates the relative entropies of the solutions with these two conformers may be determined by the solvent-solvent interactions rather than solute-solvent interactions.

### Conclusions

In studying the tGg, tGt, and gGg conformers of 1,2-ethanediol in the gas phase, it was found that these structures without intramolecular hydrogen bonds are higher in free energy by 3-4 kcal/mol than the most stable tGg' conformer. On hydration tGg is stabilized by 5.2 kcal and becomes the dominant conformer, thus the most likely conformer in aqueous solution is an O-C-C-O gauche form without intramolecular hydrogen bonding. This fits well the NMR and Raman spectroscopic experiments.

The polar groups of the solute are hydrated by five to seven water molecules and form about four hydrogen bonds with them. The most stable bonds are the nearly linear O-H(alc)···O(water) ones. Hydrogen bonds to O(alc) with donor water molecules are much more mobile. Water molecules hydrating a gauche hydroxyl group are more strongly localized than those for a trans one. The number of water molecules in the nonpolar region is insensitive to conformational changes of the solute considering rotation either about the C-C axes or about the C-O bonds.

**Acknowledgment.** We are grateful to Dr. W. L. Jorgensen for allowing the use of the BOSS program. Also we acknowledge the technical assistance of Dr. R. Goldstein and the Academic Data Network of the University of Illinois at Chicago.

Registry No. 1,2-Ethanediol, 107-21-1.

## Cyclopentadienylideneketene: Theoretical Consideration of an Infrared Spectrum Frequently Mistaken for That of Benzyne

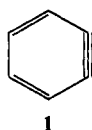
Andrew C. Scheiner<sup>†</sup> and Henry F. Schaefer III<sup>\*‡</sup>

Contribution from the National Engineering and Scientific Support Center, IBM Corporation, 1503 LBJ Freeway, Dallas, Texas 75234, and Center for Computational Quantum Chemistry, University of Georgia, Athens, Georgia 30602. Received July 25, 1991

**Abstract:** Ab initio molecular quantum mechanics has been applied to the cyclopentadienylideneketene molecule, a  $C_7H_4O$  isomer. Until very recently, it was thought that this molecule had not been observed spectroscopically. However, recent experiments appear to show that an infrared feature near  $2085\text{ cm}^{-1}$  (and often attributed to benzyne) is due to cyclopentadienylideneketene. Here the structure of the latter molecule has been optimized using three theoretical methods, including second-order perturbation theory with a triple- $\zeta$  plus double-polarization (TZ2P) basis set. Harmonic vibrational frequencies and infrared intensities have also been evaluated, and the ketene C=C plus C=O stretch is indeed consistent with the  $2085\text{-cm}^{-1}$  assignment previously identified with benzyne.

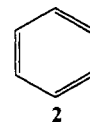
### Introduction

*o*-Benzyne has been an important molecule in the history of physical organic chemistry. Most respected contemporary organic chemistry texts<sup>1-3</sup> are in agreement, on the basis of the infrared spectrum, that the triple-bond valence structure



1

is more important than other possibilities, such as



2

The section in Vollhardt's text<sup>2</sup> entitled "Benzyne is a Strained Cycloalkyne" summarizes the current understanding.

The basis for the identification of benzyne with the triple-bond structure 1 is a series of independent experiments<sup>4-9</sup> that yielded

<sup>†</sup> IBM Corp. Present address: Biosym Technologies, Inc., 10065 Barnes Canyon Rd., San Diego, CA 92121.

<sup>‡</sup> University of Georgia.

(1) Streitwieser, A.; Heathcock, C. H. *Introduction to Organic Chemistry*, 3rd ed.; Macmillan: New York, 1985; pp 803-805.

(2) Vollhardt, K. P. C. *Organic Chemistry*; W. H. Freeman: New York, 1987; pp 925-929.

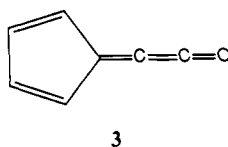
(3) March, J. *Advanced Organic Chemistry*, 3rd ed.; Wiley: New York, 1985; pp 579-587.

a value of  $\sim 2085\text{ cm}^{-1}$  for the purported  $\text{C}\equiv\text{C}$  triple-bond stretch. A carbon-carbon stretching frequency of  $2085\text{ cm}^{-1}$  falls in the normal range associated with  $\text{C}\equiv\text{C}$  triple bonds.<sup>10</sup> The first challenge to this orthodoxy came from the experimental studies of Leopold, Miller, and Lineberger,<sup>11</sup> who deduced from their laser photodetachment studies that



for benzyne is  $1860 \pm 15\text{ cm}^{-1}$ . Theory<sup>12,13</sup> subsequently provided strong support for the Lineberger assignment. In a very recent (1992) publication, Radziszewski, Hess, and Zahradnik<sup>14</sup> have reported a weak infrared feature at  $1846\text{ cm}^{-1}$  that they ascribe to benzyne. The observed IR intensity is  $2.0 \pm 0.4\text{ km/mol}$ , in perfect agreement with the 1989 prediction from theory.<sup>12</sup> Taken as a group, these studies<sup>11-14</sup> suggest that the value 2.5 is a much better estimate of the bond order of the purported "triple bond" in benzyne.

In the same time frame as the developments of the previous paragraph, several groups put forward the interpretation<sup>15-18</sup> that the observed IR feature at  $2085\text{ cm}^{-1}$  might be due not to benzyne but rather to cyclopentadienylideneketene



To readers not familiar with the benzyne literature, it may seem surprising that 3 could be mistaken in several independent spectroscopic studies for benzyne, of which it is not even an isomer. In fact, the experimental products, arising from the high-temperature pyrolysis or photolysis of phthalic anhydride or benzocyclobutenedione, were until recently of unknown mass. However, the recent work of Simon, Münzel, and Schweig<sup>18</sup> seems quite conclusive in this regard. Under the several conditions of Schweig's experiments, *o*-benzyne is always formed together with cyclopentadienylideneketene (3), and the two may be differentiated by their UV/vis absorption spectra.

Since cyclopentadienylideneketene (hereafter abbreviated as CPDK) has not been unambiguously established until very recently,<sup>16,18</sup> the purpose of the present study was to characterize this species theoretically. Questions of particular initial interest were as follows: (a) Can theory reproduce the long misidentified experimental IR feature<sup>4-9,16,18</sup> at  $2085\text{ cm}^{-1}$ ? (b) Does theory find the substantial IR intensity that has always been associated with the  $2085\text{-cm}^{-1}$  IR feature?

(4) Chapman, O. L.; Mattes, K.; McIntosh, C. L.; Pacansky, J.; Calder, G. V.; Orr, G. *J. Am. Chem. Soc.* **1973**, *95*, 6134. Chapman, O. L.; Chang, C.-C.; Kolc, J.; Rosenquist, N. R.; Tomioka, H. *J. Am. Chem. Soc.* **1975**, *97*, 6586.

(5) Dunkin, I. R.; MacDonald, J. G. *J. Chem. Soc., Chem. Commun.* **1979**, 772.

(6) Nam, H.-H.; Leroi, G. E. *J. Mol. Struct.* **1987**, *157*, 301.

(7) Wentrup, C.; Blanch, R.; Briehl, H.; Gross, G. *J. Am. Chem. Soc.* **1988**, *110*, 1874.

(8) Laing, J. W.; Berry, R. S. *J. Am. Chem. Soc.* **1976**, *98*, 660.

(9) Nam, H.-H.; Leroi, G. E. *Spectrochim. Acta, Part A* **1985**, *41*, 67.

(10) Bellamy, L. J. *The Infrared Spectra of Complex Molecules*, 2nd ed.; Chapman and Hall: London, 1980; Vol. 2.

(11) Leopold, D. G.; Miller, A. E. S.; Lineberger, W. C. *J. Am. Chem. Soc.* **1986**, *108*, 1379.

(12) Scheiner, A. C.; Schaefer, H. F.; Liu, B. *J. Am. Chem. Soc.* **1989**, *111*, 3118.

(13) Scheiner, A. C.; Schaefer, H. F. *Chem. Phys. Lett.* **1991**, *177*, 471.

(14) Radziszewski, J. G.; Hess, B. A.; Zahradnik, R. *J. Am. Chem. Soc.* **1992**, *114*, 52.

(15) Brown, R. F. C.; Browne, N. R.; Coulston, K. J.; Danen, L. B.; Eastwood, F. W.; Irvine, M. J.; Pullin, A. D. E. *Tetrahedron Lett.* **1986**, *27*, 1075.

(16) Brown, R. F. C.; Browne, N. R.; Coulston, K. J.; Eastwood, F. E.; Irvine, M. J.; Pullin, A. D. E.; Wiersum, U. E. *Aust. J. Chem.* **1989**, *42*, 1321.

(17) Schweig, A.; Münzel, N.; Meyer, H.; Heidenreich, A. *Struct. Chem.* **1990**, *1*, 89.

(18) Simon, J. G. G.; Münzel, N.; Schweig, A. *Chem. Phys. Lett.* **1990**, *170*, 187.

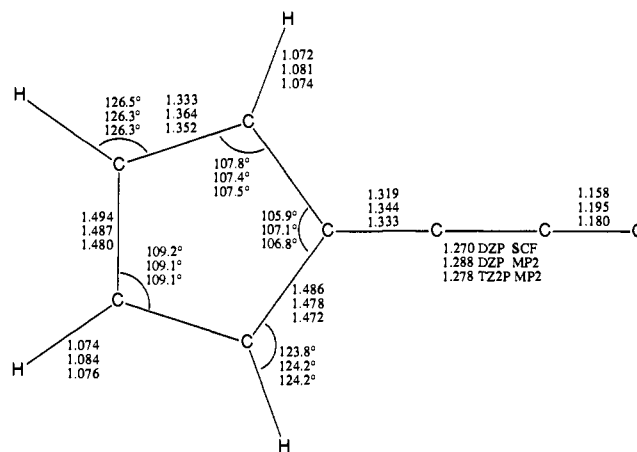


Figure 1. Predicted stationary point geometries for cyclopentadienylideneketene in  $C_{2v}$  symmetry.

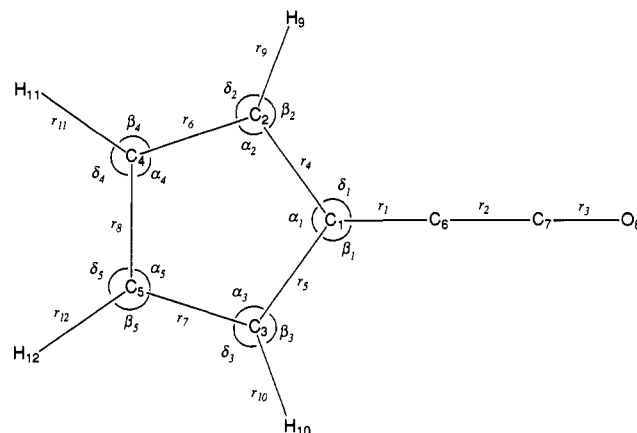


Figure 2. Definitions of internal coordinates used for the normal-coordinate analysis (Tables II and III) of the vibrations of cyclopentadienylideneketene.

### Theoretical Approach

The methods used here are comparable to those applied in our earlier studies<sup>12,13</sup> of the benzyne molecule, which has one less carbon atom and one less oxygen atom than CPDK. Specifically, both single-configuration self-consistent-field (SCF) theory and second-order perturbation theory (MP2) were used here.

The one-electron atomic basis employed initially in the present study was the standard Dunning double- $\zeta$  contraction<sup>19</sup> of Huzinaga's primitive Gaussian orbitals<sup>20</sup> (with the hydrogen *s*-functions scaled by 1.2) augmented with a single set of polarization functions at each of the atomic centers (DZP basis set). The polarization orbital exponents were chosen as  $\alpha_d(\text{C}) = 0.75$ ,  $\alpha_d(\text{O}) = 0.85$ , and  $\alpha_d(\text{H}) = 1.0$ . This DZP basis set totaled 148 atomic functions for cyclopentadienylideneketene.

Vibrational analyses have been carried out at the DZP SCF and DZP MP2 ground-state geometries, yielding harmonic frequencies and infrared absorption intensities. In the case of the SCF method, force constants and dipole derivatives were evaluated by analytic second differentiation of the energy with respect to nuclear displacements and electric field. The MP2 force constants were determined analytically,<sup>21,22</sup> and the MP2 dipole derivatives were determined via finite differences of analytically evaluated energy gradients and dipole moments.

A significantly larger basis set was also used with the MP2 method to predict the equilibrium geometry of cyclopentadienylideneketene. The triple- $\zeta$  plus double-polarization (TZ2P) basis set chosen here was the  $\text{C}(10s6p2d/5s3p2d)$ ,  $\text{H}(5s2p/3s2p)$  set of Huzinaga<sup>20</sup> and Dunning,<sup>23</sup> All six *d*-like functions were included throughout, and polarization function orbital exponents were as follows:  $\alpha_d(\text{C}) = 1.2$ ,  $0.4$ ;  $\alpha_d(\text{O}) = 1.35$ ,  $0.45$ ;  $\alpha_p(\text{H}) = 1.5$ ,  $0.5$ . The complete basis set includes 244 con-

(19) Dunning, T. H. *J. Chem. Phys.* **1970**, *53*, 2823.

(20) Huzinaga, S. *J. Chem. Phys.* **1965**, *42*, 1293.

(21) Handy, N. C.; Amos, R. D.; Gaw, J. F.; Rice, J. E.; Simandiras, E. D. *Chem. Phys. Lett.* **1985**, *120*, 151.

(22) Handy, N. C. *Int. Rev. Phys. Chem.* **1988**, *7*, 351.

(23) Dunning, T. H. *J. Chem. Phys.* **1971**, *55*, 716.

**Table I.** Symmetrized Internal Coordinates for Cyclopentadienylidene ketene<sup>a</sup>

a <sub>1</sub> Modes	
$Q_1 = r_1$	$Q_7 = (1/\sqrt{2})(r_9 + r_{10})$
$Q_2 = r_2$	$Q_8 = (1/\sqrt{2})(r_{11} + r_{12})$
$Q_3 = r_3$	$Q_9 = \alpha_1$
$Q_4 = (1/\sqrt{2})(r_4 + r_5)$	$Q_{10} = (1/2)(\beta_2 - \delta_2 + \beta_3 - \delta_3)$
$Q_5 = (1/\sqrt{2})(r_6 + r_7)$	$Q_{11} = (1/2)(\beta_4 - \delta_4 + \beta_5 - \delta_5)$
$Q_6 = r_8$	
a <sub>2</sub> Modes	
$Q_{12} = (1/\sqrt{2})(\sigma_1 - \sigma_2)$	$Q_{14} = (1/\sqrt{2})(\tau_1 + \tau_2)$
$Q_{13} = (1/\sqrt{2})(\sigma_3 - \sigma_4)$	
b <sub>1</sub> Modes	
$Q_{15} = \gamma_1$	$Q_{18} = (1/\sqrt{2})(\sigma_3 + \sigma_4)$
$Q_{16} = \gamma_2$	$Q_{19} = \sigma_5$
$Q_{17} = (1/\sqrt{2})(\sigma_1 + \sigma_2)$	$Q_{20} = (1/\sqrt{2})(\tau_1 - \tau_2)$
b <sub>2</sub> Modes	
$Q_{21} = (1/\sqrt{2})(r_4 - r_5)$	$Q_{26} = \gamma_4$
$Q_{22} = (1/\sqrt{2})(r_6 - r_7)$	$Q_{27} = (1/2)(\beta_2 - \delta_2 - \beta_3 + \delta_3)$
$Q_{23} = (1/\sqrt{2})(r_9 - r_{10})$	$Q_{28} = (1/2)(\beta_4 - \delta_4 - \beta_5 + \delta_5)$
$Q_{24} = (1/\sqrt{2})(r_{11} - r_{12})$	$Q_{29} = (1/\sqrt{2})(\alpha_2 - \alpha_3)$
$Q_{25} = \gamma_3$	$Q_{30} = (1/\sqrt{2})(\delta_1 - \beta_1)$

<sup>a</sup> Refer to Figure 2 for definitions of simple internal coordinates. Also used in this table are the following conventions:  $\sigma_1$  = angle of H<sub>9</sub>-C<sub>2</sub> out of C<sub>4</sub>-C<sub>2</sub>-C<sub>1</sub> plane,  $\sigma_2$  = angle of H<sub>10</sub>-C<sub>3</sub> out of C<sub>1</sub>-C<sub>3</sub>-C<sub>5</sub> plane,  $\sigma_3$  = angle of H<sub>11</sub>-C<sub>4</sub> out of C<sub>5</sub>-C<sub>4</sub>-C<sub>2</sub> plane,  $\sigma_4$  = angle of H<sub>12</sub>-C<sub>5</sub> out of C<sub>3</sub>-C<sub>5</sub>-C<sub>4</sub> plane,  $\sigma_5$  = angle of C<sub>6</sub>-C<sub>1</sub> out of C<sub>2</sub>-C<sub>1</sub>-C<sub>3</sub> plane,  $\tau_1$  = torsional angle between C<sub>1</sub>-C<sub>2</sub>-C<sub>4</sub> and C<sub>2</sub>-C<sub>4</sub>-C<sub>5</sub> planes,  $\tau_2$  = torsional angle between C<sub>1</sub>-C<sub>3</sub>-C<sub>5</sub> and C<sub>3</sub>-C<sub>5</sub>-C<sub>4</sub> planes,  $\gamma_1$  = out-of-plane C<sub>7</sub>-C<sub>6</sub>-C<sub>1</sub> linear bend angle,  $\gamma_2$  = out-of-plane O<sub>8</sub>-C<sub>7</sub>-C<sub>6</sub> linear bend angle,  $\gamma_3$  = in-plane C<sub>7</sub>-C<sub>6</sub>-C<sub>1</sub> linear bend angle,  $\gamma_4$  = in-plane O<sub>8</sub>-C<sub>7</sub>-C<sub>6</sub> linear bend angle.

tracted Gaussian basis functions. Considering the number of independent nuclear degrees of freedom, the MP2 geometry optimization may be one of the more challenging reported to date. In the MP2 studies, all molecular orbitals, occupied and virtual, were explicitly included. All com-

putations were carried out on the IBM 3090 E Series with vector facility, using the program CADPAC.<sup>24</sup>

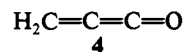
## Results and Discussion

The predicted molecular structures for CPDK in C<sub>2v</sub> symmetry are shown in Figure 1. The large-basis-set (TZ2P) results from second-order perturbation theory (MP2) should be the most reliable. The relationships among the three levels of theory are as expected.<sup>25</sup> First, all SCF bond distances are increased when electron correlation is considered via the MP2 method. Second, in going from the DZP to the significantly larger TZ2P basis set, all bond distances are decreased.

Some comparisons with the experimental equilibrium geometry<sup>26</sup> of ketene are in order. In particular, the TZ2P C=O equilibrium distance is 1.180 Å, while the comparable experimental distance for ketene is 1.161 Å. Thus it appears that the C=O bond in CPDK is slightly weaker than that of the parent ketene molecule. However, the C=C distance adjacent to the oxygen atom is predicted to be 1.278 Å (TZ2P MP2), or 0.036 Å less than that observed for ketene.<sup>26</sup> It is reasonable to conclude that this C=C bond in CPDK is stronger than that in ketene.

Prior to our discussion of vibrational frequencies, it is necessary to state precisely the symmetrized internal coordinates in which our analysis has been carried out. This information is presented in Table I and Figure 2. With these coordinates in mind, we report in Tables II and III the DZP SCF and DZP MP2 vibrational analyses of cyclopentadienylidene ketene or CPDK (3).

One of the most interesting features of Tables II and III is the fact that CPDK is not a minimum on the C<sub>7</sub>H<sub>4</sub>O potential energy hypersurface with either the DZP SCF or DZP MP2 methods. The imaginary vibrational frequency is 14i (SCF) or 118i (MP2) cm<sup>-1</sup> and leads to a bent planar equilibrium geometry. Actually, this result is not surprising, since the closely related propadienone molecule

**Table II.** Cyclopentadienylidene ketene: DZP SCF Vibrational Frequencies (cm<sup>-1</sup>), Infrared Absorption Intensities (km/mol), and Potential Energy Distributions Based on the Diagonal Elements of the Force Constant Matrix in a Basis of Symmetrized Internal Coordinates<sup>a</sup>

	theoretical harmonic freq	IR intens	PED <sup>b</sup>	mode description
a <sub>1</sub>	3442	6.3	F <sub>7</sub> (78), F <sub>8</sub> (20)	C-H str
a <sub>1</sub>	3413	5.1	F <sub>8</sub> (79), F <sub>7</sub> (-21)	C-H str
a <sub>1</sub>	2440 <sup>c</sup>	3198.5	F <sub>2</sub> (46), F <sub>3</sub> (-43), F <sub>1</sub> (-10)	ketene str
a <sub>1</sub>	1953	32.0	F <sub>1</sub> (51), F <sub>3</sub> (-30)	ketene str
a <sub>1</sub>	1719	22.8	F <sub>5</sub> (73), F <sub>9</sub> (9)	C <sub>2,3</sub> -C <sub>4,5</sub> str
a <sub>1</sub>	1507	41.2	F <sub>10</sub> (34), F <sub>11</sub> (33), F <sub>6</sub> (18), F <sub>4</sub> (-11)	H wag + ring str
a <sub>1</sub>	1271	8.4	F <sub>11</sub> (20), F <sub>2</sub> (-18), F <sub>4</sub> (16), F <sub>9</sub> (-11)	H <sub>11,12</sub> wag + C <sub>1</sub> -C <sub>2,3</sub> str + ketene str
a <sub>1</sub>	1157	0.3	F <sub>10</sub> (36), F <sub>11</sub> (-22), F <sub>4</sub> (14)	H wag + C <sub>1</sub> -C <sub>2,3</sub> str
a <sub>1</sub>	1033	11.3	F <sub>6</sub> (72), F <sub>9</sub> (8)	C <sub>4</sub> -C <sub>5</sub> str
a <sub>1</sub>	943	17.6	F <sub>4</sub> (53), F <sub>9</sub> (28), F <sub>11</sub> (13)	C <sub>1</sub> -C <sub>2,3</sub> str + C <sub>2</sub> -C <sub>1</sub> -C <sub>3</sub> bend
a <sub>1</sub>	516	0.0	F <sub>9</sub> (49), F <sub>4</sub> (-19), F <sub>1</sub> (-17), F <sub>2</sub> (-12)	C <sub>2</sub> -C <sub>1</sub> -C <sub>3</sub> bend + C <sub>1</sub> -C <sub>2,3</sub> str + ketene str
a <sub>2</sub>	1063		F <sub>13</sub> (67), F <sub>12</sub> (-20), F <sub>14</sub> (13)	H wag
a <sub>2</sub>	829		F <sub>12</sub> (66), F <sub>13</sub> (31)	H wag
a <sub>2</sub>	543		F <sub>14</sub> (82), F <sub>12</sub> (-17)	ring torsion
b <sub>1</sub>	1063	0.2	F <sub>18</sub> (49), F <sub>17</sub> (-46)	H wag
b <sub>1</sub>	896	119.5	F <sub>17</sub> (48), F <sub>18</sub> (20), F <sub>20</sub> (-17), F <sub>19</sub> (-14)	H wag + ring torsion + ketene wag
b <sub>1</sub>	725	8.9	F <sub>16</sub> (60), F <sub>15</sub> (-14), F <sub>19</sub> (-11)	O <sub>8</sub> -C <sub>7</sub> -C <sub>6</sub> bend + C <sub>7</sub> -C <sub>6</sub> -C <sub>1</sub> bend + ketene wag
b <sub>1</sub>	677	56.2	F <sub>20</sub> (37), F <sub>18</sub> (23), F <sub>19</sub> (20), F <sub>16</sub> (16)	ring torsion + H <sub>11,12</sub> wag + ketene wag + O <sub>8</sub> -C <sub>7</sub> -C <sub>6</sub> bend
b <sub>1</sub>	282	0.4	F <sub>20</sub> (37), F <sub>15</sub> (-24), F <sub>19</sub> (-22), F <sub>17</sub> (-9)	ring torsion + C <sub>7</sub> -C <sub>6</sub> -C <sub>1</sub> bend + ketene wag
b <sub>1</sub>	105	0.1	F <sub>15</sub> (46), F <sub>20</sub> (23), F <sub>19</sub> (-19)	C <sub>7</sub> -C <sub>6</sub> -C <sub>1</sub> bend + ring torsion + ketene wag
b <sub>2</sub>	3438	2.9	F <sub>23</sub> (87), F <sub>24</sub> (11)	C-H str
b <sub>2</sub>	3403	6.1	F <sub>24</sub> (88), F <sub>23</sub> (-11)	C-H str
b <sub>2</sub>	1779	0.4	F <sub>22</sub> (78), F <sub>28</sub> (-12)	C <sub>2,3</sub> -C <sub>4,5</sub> str
b <sub>2</sub>	1432	1.2	F <sub>28</sub> (36), F <sub>27</sub> (24), F <sub>21</sub> (-23), F <sub>29</sub> (15)	H wag + C <sub>1</sub> -C <sub>2,3</sub> str
b <sub>2</sub>	1274	10.6	F <sub>21</sub> (43), F <sub>29</sub> (-27), F <sub>27</sub> (18)	C <sub>1</sub> -C <sub>2,3</sub> str + C <sub>1</sub> -C <sub>2,3</sub> -C <sub>4,5</sub> bend
b <sub>2</sub>	1192	10.8	F <sub>28</sub> (32), F <sub>27</sub> (-31), F <sub>22</sub> (16), F <sub>29</sub> (-15)	H wag + C <sub>2,3</sub> -C <sub>4,5</sub> str + C <sub>1</sub> -C <sub>2,3</sub> -C <sub>4,5</sub> bend
b <sub>2</sub>	833	1.1	F <sub>29</sub> (57), F <sub>21</sub> (34)	C <sub>1</sub> -C <sub>2,3</sub> -C <sub>4,5</sub> bend + C <sub>1</sub> -C <sub>2,3</sub> str
b <sub>2</sub>	543	32.5	F <sub>26</sub> (97)	O <sub>8</sub> -C <sub>7</sub> -C <sub>6</sub> bend
b <sub>2</sub>	438	14.9	F <sub>30</sub> (67), F <sub>29</sub> (-10)	ketene wag + C <sub>1</sub> -C <sub>2,3</sub> -C <sub>4,5</sub> bend
b <sub>2</sub>	-14	2.8	F <sub>26</sub> (51), F <sub>25</sub> (-48)	ketene bend

<sup>a</sup> See Table I for definitions of internal coordinates. <sup>b</sup> Dominant contributions to diagonal potential energy distribution; sign indicates phase of displacement relative to the defined symmetrized internal coordinates. <sup>c</sup> Experimental fundamental equals 2085 cm<sup>-1</sup>.<sup>16,18</sup>

**Table III.** Cyclopentadienyldeneketene: DZP MP2 Vibrational Frequencies ( $\text{cm}^{-1}$ ), Infrared Absorption Intensities ( $\text{km/mol}$ ), and Potential Energy Distributions Based on the Diagonal Elements of the Force Constant Matrix in a Basis of Symmetrized Internal Coordinates<sup>a</sup>

	theoretical harmonic freq	IR intens	PED <sup>b</sup>	mode description
a <sub>1</sub>	3324	6.7	F <sub>7</sub> (75), F <sub>8</sub> (24)	C-H str
a <sub>1</sub>	3296	2.8	F <sub>8</sub> (75), F <sub>9</sub> (-25)	C-H str
a <sub>1</sub>	2301 <sup>c</sup>	1016.5	F <sub>2</sub> (49), F <sub>3</sub> (-40), F <sub>1</sub> (-11)	ketene str
a <sub>1</sub>	1770	24.3	F <sub>1</sub> (50), F <sub>3</sub> (-31)	ketene str
a <sub>1</sub>	1543	13.8	F <sub>5</sub> (69), F <sub>9</sub> (10)	C <sub>2,3</sub> -C <sub>4,5</sub> str
a <sub>1</sub>	1404	41.9	F <sub>11</sub> (32), F <sub>10</sub> (32), F <sub>6</sub> (21), F <sub>4</sub> (-11)	H wag + ring str
a <sub>1</sub>	1174	2.6	F <sub>11</sub> (21), F <sub>4</sub> (17), F <sub>2</sub> (-15), F <sub>3</sub> (-11)	H <sub>11,12</sub> wag + C <sub>1</sub> -C <sub>2,3</sub> str + ketene str
a <sub>1</sub>	1078	2.9	F <sub>10</sub> (30), F <sub>11</sub> (-22), F <sub>4</sub> (20)	H wag + C <sub>1</sub> -C <sub>2,3</sub> str
a <sub>1</sub>	996	7.1	F <sub>6</sub> (60), F <sub>9</sub> (13), F <sub>10</sub> (-12)	C <sub>4</sub> -C <sub>5</sub> str
a <sub>1</sub>	891	8.5	F <sub>4</sub> (45), F <sub>9</sub> (30), F <sub>11</sub> (16)	C <sub>1</sub> -C <sub>2,3</sub> str + C <sub>2</sub> -C <sub>1</sub> -C <sub>3</sub> bend
a <sub>1</sub>	481	0.2	F <sub>9</sub> (47), F <sub>1</sub> (-18), F <sub>4</sub> (-16), F <sub>2</sub> (-13)	C <sub>2</sub> -C <sub>1</sub> -C <sub>3</sub> bend + C <sub>1</sub> -C <sub>2,3</sub> str + ketene str
a <sub>2</sub>	889		F <sub>13</sub> (62), F <sub>12</sub> (-24), F <sub>14</sub> (14)	H wag
a <sub>2</sub>	696		F <sub>12</sub> (52), F <sub>13</sub> (39), F <sub>14</sub> (8)	H wag
a <sub>2</sub>	487		F <sub>14</sub> (77), F <sub>12</sub> (-23)	ring torsion
b <sub>1</sub>	899	0.3	F <sub>17</sub> (50), F <sub>18</sub> (-45)	H wag
b <sub>1</sub>	772	92.7	F <sub>17</sub> (48), F <sub>20</sub> (19), F <sub>18</sub> (19), F <sub>19</sub> (-13)	H wag + ring torsion + ketene wag
b <sub>1</sub>	625	7.6	F <sub>20</sub> (28), F <sub>19</sub> (24), F <sub>18</sub> (19), F <sub>16</sub> (-18)	ring torsion + ketene wag + H <sub>11,12</sub> wag + O <sub>8</sub> -C <sub>7</sub> -C <sub>6</sub> bend
b <sub>1</sub>	603	34.9	F <sub>16</sub> (59), F <sub>20</sub> (21), F <sub>18</sub> (11)	O <sub>8</sub> -C <sub>7</sub> -C <sub>6</sub> bend + ring torsion
b <sub>1</sub>	253	1.3	F <sub>20</sub> (33), F <sub>19</sub> (-25), F <sub>15</sub> (-25), F <sub>17</sub> (-10)	ring torsion + ketene wag + C <sub>7</sub> -C <sub>6</sub> -C <sub>1</sub> bend
b <sub>1</sub>	95	0.1	F <sub>15</sub> (47), F <sub>20</sub> (22), F <sub>19</sub> (-18)	C <sub>7</sub> -C <sub>6</sub> -C <sub>1</sub> bend + ring torsion + ketene wag
b <sub>2</sub>	3321	1.4	F <sub>23</sub> (86), F <sub>24</sub> (13)	C-H str
b <sub>2</sub>	3284	4.8	F <sub>24</sub> (86), F <sub>23</sub> (-13)	C-H str
b <sub>2</sub>	1602	0.3	F <sub>22</sub> (74), F <sub>28</sub> (-15)	C <sub>2,3</sub> -C <sub>4,5</sub> str
b <sub>2</sub>	1324	2.7	F <sub>28</sub> (33), F <sub>27</sub> (25), F <sub>21</sub> (-24), F <sub>29</sub> (14)	H wag + C <sub>1</sub> -C <sub>2,3</sub> str
b <sub>2</sub>	1189	15.6	F <sub>21</sub> (45), F <sub>29</sub> (-26), F <sub>27</sub> (17)	C <sub>1</sub> -C <sub>2,3</sub> str + C <sub>1</sub> -C <sub>2,3</sub> -C <sub>4,5</sub> bend
b <sub>2</sub>	1105	11.7	F <sub>28</sub> (31), F <sub>27</sub> (-30), F <sub>22</sub> (18), F <sub>29</sub> (16)	H wag + C <sub>2,3</sub> -C <sub>4,5</sub> str + C <sub>1</sub> -C <sub>2,3</sub> -C <sub>4,5</sub> bend
b <sub>2</sub>	780	0.1	F <sub>29</sub> (59), F <sub>21</sub> (32)	C <sub>1</sub> -C <sub>2,3</sub> -C <sub>4,5</sub> bend + C <sub>1</sub> -C <sub>2,3</sub> str
b <sub>2</sub>	455	3.7	F <sub>26</sub> (86), F <sub>30</sub> (-8)	O <sub>8</sub> -C <sub>7</sub> -C <sub>6</sub> bend
b <sub>2</sub>	347	19.0	F <sub>30</sub> (50), F <sub>26</sub> (38)	ketene wag + O <sub>8</sub> -C <sub>7</sub> -C <sub>6</sub> bend
b <sub>2</sub>	118i	5.1	F <sub>26</sub> (63), F <sub>25</sub> (19), F <sub>30</sub> (16)	ketene bend

<sup>a</sup> See Table I for definitions of internal coordinates. <sup>b</sup> Dominant contributions to diagonal potential energy distribution; sign indicates phase of displacement relative to the defined symmetrized internal coordinates. <sup>c</sup> Experimental fundamental equals  $2085 \text{ cm}^{-1}$ .<sup>16,18</sup>

displays exactly the same behavior.<sup>27</sup> Propadienone, according to Farnell and Radom,<sup>28</sup> is significantly bent about the C=C=C angle ( $145^\circ$ ), but only slightly bent about the C=C=O angle ( $170^\circ$ ).

CPDK is slightly different from **4**, since propadienone is predicted to have  $C_{2v}$  symmetry from SCF theory and only gives the correct bent planar structure<sup>27</sup> when electron correlation is explicitly considered.<sup>28</sup> Both the SCF and MP2 structures for CPDK are bent planar. However, for CPDK the extent of bending, as predicted from the magnitude of the imaginary vibrational frequency, is much less from SCF theory ( $14i \text{ cm}^{-1}$ ) than from MP2 ( $118i \text{ cm}^{-1}$ ). Thus the qualitative effect of electron correlation is the same for propadienone<sup>28</sup> and for CPDK.

Although our three  $C_{2v}$  structures are transition states, the theoretical vibrational frequencies should be very similar to those for the bent planar equilibrium geometry. Due to the extraordinary flatness of the transition-state reaction coordinate, all but this one vibrational degree of freedom should be reliably simulated by the  $C_{2v}$  symmetry results.

Only one fundamental vibrational frequency for CPDK seems to be unequivocally established, namely that at about  $2085 \text{ cm}^{-1}$ , from the Australian group<sup>16</sup> and from the German group.<sup>18</sup> The DZP SCF harmonic prediction for this fundamental is  $2440 \text{ cm}^{-1}$ , and the DZP MP2 prediction is  $2301 \text{ cm}^{-1}$ . These theoretical predictions lie respectively 17.0% and 10.3% above experimental results. The former error seems somewhat high for the DZP SCF method,<sup>29</sup> but the latter falls in an acceptable relationship with

experimental results. Table III shows that the DZP MP2 harmonic vibrational frequency is 49% ketene C=C and 40% ketene C=O in character.

More significantly, the theoretical IR intensities for this C=C plus C=O stretch are enormous (3199 and 1016  $\text{km/mol}$ , respectively, for the DZP SCF and DZP MP2 methods). These large IR intensities are fully consistent with the preferential observation of this C=C plus C=O stretching fundamental of cyclopentadienyldeneketene. Note particularly the immense difference between these IR intensities and the 2  $\text{km/mol}$  predicted<sup>12,13</sup> and subsequently observed<sup>14</sup> for



in benzyne. Thus we have complete resolution of the long-standing problem of this puzzling IR feature observed at  $2085 \text{ cm}^{-1}$ .

More generally, the SCF and MP2 vibrational frequencies for CPDK fall in the expected relationship. In fact, every one of the 29 real harmonic vibrational frequencies is predicted to decrease from SCF to MP2. There are, however, some notable differences in theoretical IR intensities. Already mentioned was the factor of 3 decrease (SCF to MP2) in the IR intensity of the fundamental observed at  $2085 \text{ cm}^{-1}$ .

For example, the MP2 a<sub>1</sub> frequency at  $1174 \text{ cm}^{-1}$  has SCF and MP2 intensities of 8.4 and 2.6  $\text{km/mol}$ , respectively. For the MP2 a<sub>1</sub> mode predicted at  $1078 \text{ cm}^{-1}$ , the SCF IR intensity of only 0.3  $\text{km/mol}$  is increased to 2.9  $\text{km/mol}$  with MP2. The largest percentage change in IR intensities occurs for the b<sub>2</sub> mode predicted from DZP MP2 to be  $\omega = 455 \text{ cm}^{-1}$ . The SCF IR intensity is large (32.5  $\text{km/mol}$ ), while the MP2 prediction is only 3.7  $\text{km/mol}$ . The above few exceptions again prove the rule that theoretical IR intensities can be very sensitive to level of theory.<sup>30</sup>

(24) Amos, R. D.; Rice, J. E. CADPAC: The Cambridge Analytic Derivatives Package, Issue 4.0. Cambridge University, 1987.

(25) Schaefer, H. F. Status of *Ab Initio* Molecular Structure Predictions. In *Critical Evaluation of Chemical and Physical Structural Information*; Lide, D. R., Paul, M. A., Eds.; National Academy of Sciences: Washington, DC, 1974; pp 591-602.

(26) Duncan, J. L.; Munroe, B. J. *Mol. Struct.* **1987**, *161*, 311.

(27) Brown, R. D.; Godfrey, P. D.; Champion, R.; McNaughton, D. J. *Am. Chem. Soc.* **1981**, *103*, 5711.

(28) Farnell, L.; Radom, L. *Chem. Phys. Lett.* **1982**, *91*, 373.

(29) Besler, B. H.; Scuseria, G. E.; Scheiner, A. C.; Schaefer, H. F. *J. Chem. Phys.* **1988**, *89*, 360.

(30) Yamaguchi, Y.; Frisch, M. J.; Gaw, J. F.; Schaefer, H. F.; Binkley, J. S. *J. Chem. Phys.* **1986**, *84*, 2262.

Since the observed fundamental at 2085  $\text{cm}^{-1}$  is a mixture of ketene-like C=C and C=O stretches, it is of interest to see what other fundamentals these two internal coordinates affect. The remainder of the C=O stretch goes primarily (i.e., 31%) into the  $a_1$  mode predicted at 1770  $\text{cm}^{-1}$  (DZP MP2). If we decrease this theoretical harmonic frequency for anharmonicity, basis set, and higher level correlation effects, the fundamental vibrational frequency may be estimated to be about 1650  $\text{cm}^{-1}$ . Note that the IR intensity of this fundamental is predicted to be substantial, 24  $\text{km/mol}$ , but nothing like the 1017  $\text{km/mol}$  of the feature observed near 2085  $\text{cm}^{-1}$ .

A final point of particular interest is the feature at 2093  $\text{cm}^{-1}$  long assigned<sup>5</sup> to the C=C stretch of perdeuterated benzyne. Note that in an  $\text{N}_2$  matrix at 12 K, the shift in this frequency was determined by Dunkin and MacDonald to be 2093 - 2084 = 9  $\text{cm}^{-1}$ . It would not be surprising at this point to conclude that this feature is instead a ketene-like fundamental of perdeuterated CPDK. However, this harmonic vibrational frequency is predicted to be red-shifted by 0.5  $\text{cm}^{-1}$  at the DZ+P SCF level of theory and by 0.3  $\text{cm}^{-1}$  with the DZ+P MP2 method. Thus we must be very cautious in assigning the experimental IR feature at 2093  $\text{cm}^{-1}$ . New experiments might be very helpful in this regard.

### Concluding Remarks

This work provides a complete theoretical prediction of the harmonic vibrational frequencies and infrared intensities of the cyclopentadienylideneketene molecule (**3**). Until recently<sup>16,18</sup> there was no evidence that this molecule had been observed spectro-

scopically. However the theoretical normal mode that is 49% ketene C=C stretch and 40% C=O stretch is predicted to have a remarkably strong IR intensity. These predictions are consistent with the observed IR feature at 2085  $\text{cm}^{-1}$ , which was for many years assumed to be due to the C=C stretch in benzyne.

Further experimental studies of **3** would be of great value, as this new molecule becomes of interest in its own right. An obvious question yet to be resolved is whether some of the other fundamentals previously assigned<sup>4-9</sup> to benzyne are in fact due to cyclopentadienylideneketene. For cyclopentadienylideneketene (**3**) the next most intense IR feature is predicted at 772  $\text{cm}^{-1}$  (harmonic vibrational frequency,  $b_1$  symmetry, intensity 92.7  $\text{km/mol}$ , DZP MP2). This theoretical result fits well with the observed "benzyne" feature<sup>4</sup> at 736  $\text{cm}^{-1}$ , which is the strongest experimental IR feature after that at 2085  $\text{cm}^{-1}$ . Unfortunately, this interpretation is muddled by the fact that benzyne itself has its very strongest IR fundamental predicted at 751  $\text{cm}^{-1}$  ( $b_1$  symmetry, 85.8  $\text{km/mol}$ , DZP MP2). Thus the theoretical predictions for either cyclopentadienylideneketene or benzyne can accommodate the intense IR feature observed at 736  $\text{cm}^{-1}$ .

**Acknowledgment.** This research was supported by the U.S. Department of Energy, Office of Basic Energy Sciences, Division of Chemical Sciences, Fundamental Interactions Branch (Grant DE-FG09-87ER13811). We thank Drs. Mary M. Gallo and Yaoming Xie for helpful discussions.

**Registry No.** Cyclopentadienylideneketene, 115252-80-7.

## Calculation of the Relative Binding Free Energy of Three Inhibitors of the Photosynthetic Reaction Center of *Rhodospseudomonas viridis* Using the Molecular Dynamics/Free Energy Perturbation Method

John E. Mertz,<sup>†</sup> Jan W. Andzelm,<sup>†</sup> Detlef Labrenz,<sup>‡</sup> and Ursula Egner\*<sup>§</sup>

Contribution from Cray Research, Inc., 655E Lone Oak Drive, Eagan, Minnesota 55120, Cray Research GmbH, Kistlerhofstrasse 168, D-8000 München 70, Germany, and Schering AG, Müllerstrasse 170-178, D-1000 Berlin 65, Germany. Received September 9, 1991

**Abstract:** The results of the relative changes in binding free energy between the complex of the bacterial photosynthetic reaction center (RC) of *Rhodospseudomonas viridis* with inhibitors ametryn, atraton, and prometon are presented. These results were determined by using molecular dynamics, free energy perturbation methods. Force field parameters for the cofactors and non-heme iron of the RC along with the inhibitors are developed from a combination of quantum mechanical calculations and previous spectroscopic and molecular modeling studies. The calculated free energy changes compare well with the measured data and lie within the error limits of this method. The calculations yielded a ranking of the relative stabilities of the inhibitors as atraton < prometon < ametryn. The relative free energy of solvation and the relative free energy of the complexes between the inhibitors and the RC both favor a hydrophobic substituent for better binding.

### Introduction

The photosynthetic reaction center (RC) complexes provide model systems for rationalizing the ability of various herbicides to inhibit photosynthesis. RCs have been purified from numerous species of bacteria, and the X-ray structures of the RCs of *Rhodospseudomonas viridis* (*Rps. viridis*) and *Rhodobacter sphaeroides* (*Rb. sphaeroides*) have been solved to high resolution.<sup>1-3</sup> RCs from many species are composed of three protein subunits (L, M, and H), four bacteriochlorophylls, two bacter-

iopeophytins, two quinones ( $Q_A$  and  $Q_B$ ), and one non-heme iron atom. In the case of the RC of *Rps. viridis*, a cytochrome with four heme molecules is also present. Since the elucidation of the X-ray structure of these RCs, several calculations have been carried out that relate their structure and function. Simulations of optical spectra were performed including absorption, light-induced absorbance changes, and circular dichroism.<sup>4-7</sup> The

(1) Deisenhofer, J.; Epp, O.; Miki, K.; Huber, R.; Michel, H. *Nature* **1985**, *318*, 618.

(2) Allen, J. P.; Feher, G.; Yeates, T. O.; Komiyama, H.; Rees, D. C. *Proc. Natl. Acad. Sci. U.S.A.* **1988**, *85*, 8487.

(3) Creighton, S.; Hwang, J.-K.; Warshel, A.; Parson, W. W.; Norris, J. *Biochemistry* **1988**, *27*, 774.

<sup>†</sup>Cray Research, Inc.

<sup>‡</sup>Cray Research GmbH.

<sup>§</sup>Schering AG.